LBNL-5685E

ERNEST ORLANDO LAWRENCE
BERKELEY NATIONAL LABORATORY

Self-organization and self-limitation in high power impulse magnetron sputtering

A. Anders
Lawrence Berkeley National Laboratory

Windows and Envelope Materials Group
Building Technology and Urban Systems Department
Environmental Energy Technologies Division

April 2012

Published in *Applied Physics Letters*. 100, 224104 (2012)

LBNL-5685E

Submitted to

Applied Physics Letters

Assigned manuscript # L12-04454R

revised version submitted 2012-04-25

accepted 2012-05-16

published as

Appl. Phys. Lett. **100**, 224104 (2012)

http://link.aip.org/link/doi/10.1063/1.4724205

Self-organization and self-limitation in high power impulse magnetron sputtering

André Anders

Lawrence Berkeley National Laboratory, Berkeley, California

email: aanders@lbl.gov

ACKNOWLEDGMENT

Pavel Ni and Albert Rauch are gratefully acknowledged for being key on imaging the ionization zones shown in Fig. 1. I thank Rueben Mendelsberg for his comments. This work was supported by the Assistant Secretary for Energy Efficiency and Renewable Energy, Office of Building Technology of the U.S. Department of Energy (DOE) under Contract No. DE-AC02-05CH11231.

Self-organization and self-limitation in high power impulse magnetron sputtering

André Anders[a)]

Lawrence Berkeley National Laboratory, Berkeley, California

The plasma over the racetrack in high power impulse magnetron sputtering (HiPIMS) develops in traveling ionization zones. Power densities can locally reach 10^9 W/m^2, which is much higher than usually reported. Ionization zones move because ions are "evacuated" by the electric field, exposing neutrals to magnetically confined, drifting electrons. Drifting secondary electrons amplify ionization of the *same* ionization zone where the primary ions came from, while sputtered and outgassing atoms are supplied to the *following* zone(s). Strong density gradients parallel to the target disrupt electron confinement: a negative feedback mechanism that stabilizes ionization runaway.

PACS numbers: 52.25.-b, 52.25.Jm, 52.35.Qz, 52.70.Kz, 52.80.Sm

[a)] Electronic mail: *aanders@lbl.gov*

Conventional magnetron sputtering delivers only a very small flux of ions to the substrate. To enhance the flux of ions for ion-assisted deposition, the magnetron discharge can be operated with pulses of very high power, typically with a nominal, target-area-averaged peak power density of about 10^7 W/m^2, which is known as *high power impulse magnetron sputtering* (HiPIMS).[1-3]

Magnetron discharges are based on a closed drift of magnetically confined energetic electrons capable of causing ionizing collisions, creating a zone of enhanced plasma density. Beneath the dense plasma, the target is strongly eroded by sputtering, forming the so-called erosion "racetrack." The physics discussed here applies regardless of the shape of the target and racetrack. It also applies if the erosion zone is smeared out, i.e., in the case of magnetrons with rotating targets or rotating magnets.[4,5] At high power, the magnetron discharge has the capability for self-sputtering and ionization runway.[6,7] The presence of noble gas such as argon can lead to an additional plasma density enhancement through a "gas recycling" loop in front of the target in analogy to a self-sputtering / ionization loop.[8] Taking all types of gas and metal fluxes into account is important since they determine the density of neutrals that are available for ionization.

Recent fast camera observations of HiPIMS discharges revealed that the plasma over the racetrack is not uniformly distributed but concentrated in dense, more-or-less regularly spaced plasma zones.[9-11] The dense plasma zones move in the $\mathbf{E}\times\mathbf{B}$ direction with typically 10^4 m/s which is only a fraction of the electrons' drift velocity (~ 10^5 m/s). It was suggested that the moving dense plasma zones are better described as moving ionization zones since it is not the plasma itself that is moving but the location of most intense ionization.[10] Fig. 1 shows examples

of such ionization zones at different stages of their evolution. Such images suggest that it takes time and/or a certain power density for the localized zones to develop, and that they are affecting each other, sometimes forming symmetrical, self-organized patterns.

In this contribution, the underlying reasons for the formation, motion, self-organization, and self-limitation of the ionization zones are analyzed. It is argued that the localization of dense plasma is at the very heart of HiPIMS operation in terms of enabling the observed high discharge currents and high degree of ionization.

In a previous publication,[10] the formation of highly localized ionization zones was explained by considering the path of electrons and their likelihood of causing ionization. The actual path of electrons is complicated since the electron motion occurs in non-parallel and non-uniform electric and magnetic fields. Between collisions, electron motion is governed by acceleration in the local electric field and gyration around magnetic field lines caused by the Lorentz force leading to the equation of motion $m_e\, d\mathbf{v}/dt = -e\left(\mathbf{E} + \mathbf{v}\times\mathbf{B}\right)$, where m_e is the electron mass, **v** is the velocity vector, e is the elementary charge, and **E** and **B** are the vectors of the electric field and magnetic induction respectively. One conventionally averages over the gyration motion and the oscillating motion of the gyration center. The remaining motion is the closed electron drift, most notably the $\mathbf{E}\times\mathbf{B}$, $\mathbf{B}\times\nabla B$ and higher order drifts, which are additive.[12] For simplicity, we refer to the "$\mathbf{E}\times\mathbf{B}$ drift" but understand that other drift components are also present.

It was proposed[10] that the likelihood of ionization by electron impact is subject to a positive feedback mechanism. Under typical magnetron conditions, electrons travel a long path before making an ionizing collision. When a drifting energetic electron encounters a region of somewhat higher density of particles, it is more likely to interact in this region, as is clear from the mean free path formula $\lambda_e^{-1} = \sum_p \sigma_{ep} n_p$, where n_p is the density of particles of type p, and $\sigma_{ep}(v)$ is the velocity-dependent interaction cross section between the electron and particle of type p. Interaction of energetic secondary electrons will lead to dissipation of energy in the region of enhanced particle density, promoting an increase in ionization, and thereby further enhancing the plasma density at this location. This, in turn, increases the chance that other drifting energetic electrons arriving at the denser zone interact with ions and electrons and transfer their energy. Therefore, a density fluctuation has the capability to develop into a dense plasma zone since its electron "stopping power" increases as the density increases.

To go beyond this conceptual explanation one needs to consider the underlying mechanism responsible for the motion of the ionization zone, formation of plasma patterns and self-limitation of the ionization runaway. Suppose an ion is formed at a distance d over the racetrack. Since ions are not magnetized we can neglect the influence of the magnetic field on their trajectory: the equation of ion motion reads $d\mathbf{v}_i/dt = \left(Qe/m_i\right)\mathbf{E}$, where Q is the ion charge state number (in most cases $Q = 1$). The electric field over the racetrack accelerates ions towards the racetrack, as is known from measurements of the plasma potential distribution.[13,14] That means that the ion is "evacuated" from the location of ionization. Drifting electrons arriving a bit later do not find a neutral (since it was ionized) or ion anymore (since the electric field removed it). Therefore, later arriving electrons drift further along the racetrack until they find

particles to interact with. This implies a drift of the ionization location in the $\mathbf{E}\times\mathbf{B}$ direction, in agreement with observation.[9-11] The speed of the ionization zone is determined by how fast the ions are evacuated by the electric field.

If we designate ξ to be the coordinate along the racetrack, the velocity of the ionization zone (IZ) can be written as $v_{IZ} = d\xi_{IZ}/dt$. Assuming an approximately constant velocity of the ionization front, one can write

$$v_{IZ} \approx \Delta\xi_{IZ}/\Delta t_i \tag{1}$$

where $\Delta\xi_{IZ}$ is the thickness the ionization zone (slab) that is approximately simultaneously ionized by drifting energetic electrons, and Δt_i is the time it takes to evacuate the slab of ions. We should recall that the electrons are actually gyrating around magnetic field lines, which are perpendicular to the $\mathbf{E}\times\mathbf{B}$ direction, i.e. perpendicular to ξ. Therefore one should expect that the ionization zone edge is perpendicular to ξ and any process in the ξ-direction is smeared out by at least two times the electron gyration radius, i.e. by

$$\Delta\xi_{IZ} \approx 2r_{g,e} = \frac{2m_e u_{e\perp}}{eB} \tag{2}$$

The electron velocity perpendicular to the magnetic field direction has an upper limit given by the applied voltage (most of it drops in the thin sheath next to the target), $u_{e\perp} \approx \left(2eV_{sheath}/m_e\right)^{1/2}$. Therefore,

$$\Delta\xi_{IZ} \approx \left(\frac{8V_{sheath}}{B^2}\frac{m_e}{e}\right)^{1/2} \tag{3}$$

To estimate how long it takes for an ion to reach the target surface, we can divide the path from the ionization location to the target surface in two segments; one is the magnetic presheath, the other is the sheath itself. The sheath is much thinner than the magnetic presheath, and the ion velocity in the sheath is much higher, therefore, the evacuation time is dominated by the ion travel time in the magnetic presheath. If we assume that *d* is the distance between ionization location and the target surface, and if we further assume that the electric field in the magnetic presheath can be approximated by an average value, E_{mps}, the evacuation time can be readily estimated by

$$\Delta t_i \approx \left(\frac{2d}{E_{mps}}\frac{m_i}{Qe}\right)^{1/2} \tag{4}$$

Inserting (3) and (4) into (1) gives

$$v_{IZ} = \frac{2}{B}\left(\frac{QV_{sheath}E_{mps}}{d}\frac{m_e}{m_i}\right)^{1/2} \tag{5}$$

We compare this now with data from experiments:[10,13] $B \approx 60\,\mathrm{mT}$, $Q = 1$, $V_{sheath} \approx 400\,\mathrm{V}$, $E_{mps} \approx 5\times10^{4}\,\mathrm{V/m}$, $m_i(Nb) = 93\times1.66\times10^{-27}\,\mathrm{kg}$, $m_i(Ar) = 40\times1.66\times10^{-27}\,\mathrm{kg}$, $m_e = 9.1\times10^{-31}\,\mathrm{kg}$, $d \approx 2\,\mathrm{mm}$, giving about $\Delta t_i = 0.2 - 0.3\,\mu\mathrm{s}$ and $v_{IZ} \approx 10^{4}\,\mathrm{m/s}$. Such ionization front velocity is in agreement with observations.[9-11] From (5) we expect that the velocity of the ionization zone motion is smaller when the mass of ions is greater. This, too, is in agreement with experiments.[10] Lack of precise data and the fact that more than one type of ions is involved makes comparison difficult.

Once the ions arrive at the target surface, they become neutralized and cause sputtering of surface atoms as well as emission of secondary electrons. Depending on the type of ions, they may either stay with the target, or, like in the case of noble gas ions, return as neutrals to the region above the target. Therefore, generally, we need to consider fluxes of both sputtered atoms and gas atoms when discussing the evolution of the neutral density distribution.[8] After ion impact, it takes time for the neutrals to move from the surface to the region where they could be ionized by the drifting energetic electrons. This is typically only $d = 1-3\,\mathrm{mm}$ from the target, as side-on images of the magnetron plasma indicate.[10] Sputtered atoms have a Thompson energy distribution[15,16]

$$f_{\mathrm{Thompson}}(\varepsilon) \propto \frac{\varepsilon}{(\varepsilon + \varepsilon_{SB})^{3}} \tag{6}$$

where ε_{SB} is the binding energy of the target surface atoms. The distribution (6) has a peak at $\varepsilon_{SB}/2$ and falls with ε^{-2}. The most likely time for a sputtered atom to move the distance d is therefore

$$\Delta t_{sputter} \geq d/v_{sputter} = d\Big/\left(\varepsilon_{SB}/m_{sputter}\right)^{1/2} \tag{7}$$

where the "greater than" case accounts for collisions that slow down sputtered atoms. A small fraction of the arriving ions may be backscattered from the target as very energetic neutrals. Most ions, however, are subplanted beneath the target surface and, in case of noble gases, outgas and leave the target with a very low energy corresponding to the temperature of the target surface. Hence the time is much longer for those atoms to reach the ionization region:

$$\Delta t_{gas} = d/v_{gas} = d\Big/\left(kT_{\mathrm{target}}/m_{gas}\right)^{1/2} \tag{8}$$

It should be noted that several percent of noble gas ions may be trapped below the surface and reach the surface by radiation enhanced diffusion.[5] Some trapped noble gas atoms could be collisionally mobilized close to the surface and receive additional kinetic energy when being pushed out from the lattice.[5] In this sense, sputtered noble gas atoms can be treated like sputtered target atoms but with their different mass. The appearance of atoms with different velocities smears out the timing when neutrals become available for ionization after ion evacuation. The temporary lack of neutrals and ions is evident by the dark wake left behind the sharp density edge of an ionization zone.

Using again the case of niobium sputtered in argon, with $\varepsilon_{SB}(Nb) = 5.93\,\mathrm{eV}$ (ref.[17]) and estimate $T_{\mathrm{target}} \approx 10^3\,\mathrm{K}$, we arrive at about $\Delta t_{sputter}(Nb) \geq 0.8\,\mu\mathrm{s}$ and $\Delta t_{gas}(Ar) \approx 4\,\mu\mathrm{s}$. Since the ionization front moves with about 10^4 m/s, it moves about 10 mm and 50 mm in the characteristic times $(\Delta t_i + \Delta t_{sputter}) \approx 1\,\mu\mathrm{s}$ (for Nb) and $(\Delta t_i + \Delta t_{gas}) \approx 5\,\mu\mathrm{s}$ (for Ar), respectively. These characteristic times and lengths lead to important conclusions. Neutrals produced by sputtering and outgassing do not contribute to the ionization runaway of the particular ionization zone the ions were originating from. Instead, they contribute to the *following ionization zones*, i.e. ionization zones that appear later at this location. In contrast, the secondary electrons, drifting faster than the ionization zone, are able to catch up with the *same* ionization zone where the primary ions came from. A dense plasma zone amplifies itself through the secondary electron mechanism, and it provides a delayed cloud of neutrals to the following ionization zone.

The feedback circles shown in previous HIPIMS publications[7,8,18] do not indicate any spatial separation of secondary electrons and neutrals emitted by the target surface; they are one-dimensional and therefore oversimplified. The movement of the ionization front parallel to the target surface and the delayed availability of neutrals in the feedback system shows that the ionization probability, and thus plasma density, of an ionization zone depends on the ionization of the *preceding* ionization zone. This is the mechanism for self-organization of ionization zones.

The ionization rate

$$\left(\frac{\partial n_i}{\partial t}\right)_{ionization} = K_\alpha n_a n_e \tag{9}$$

depends equally on the density of electrons and neutrals, where

$$K_\alpha = \int f_e(\varepsilon)\, \varepsilon^{1/2}\, \sigma_{ea}(\varepsilon)\, d\varepsilon \tag{10}$$

is the ionization rate coefficient, containing the electron energy distribution function $f_e(\varepsilon)$ and the ionization cross section $\sigma_{ea}(\varepsilon)$. Typically, three different groups of neutrals are involved: (i) neutrals from the gas background, (ii) sputtered atoms, (iii), outgassing / returning gas from the target. Therefore, the appearance of self-organized plasma zones should depend on the supply of each of the types of neutrals. The distance between two ionization zones A and B is largely given by the appearance of neutrals from the target, i.e.,

$$\Delta\xi_{AB} = \begin{cases} v_{IZ}\,(\Delta t_i + \Delta t_{sputter}) & \text{for self-sputtering} \\ v_{IZ}\,(\Delta t_i + \Delta t_{gas}) & \text{for gas sputtering} \end{cases} \tag{11}$$

leading to the above-mentioned 10 mm and 50 mm, respectively. As more than one species of atoms are involved, a superposition of density waves of different neutral particles can be expected, which prevents maintaining a simple, fully symmetrical self-organized pattern. Rather, generally, one should expect changes and evolution of patterns as time elapses within a HiPIMS pulse. For example, considering experiments[10,11] with a small magnetron having a

racetrack circumference of about 50 mm, the above estimate suggest that up to 5 ionization zones exist. A changing pattern should be expected when the ratio $\left(\Delta t_i + \Delta t_{gas}\right)\big/\left(\Delta t_i + \Delta t_{sputter}\right)$ is not an integer number. Additionally, background gas is source of neutrals, and one should expect more ionization zones as the background pressure is increased.

The high likelihood that drifting electrons interact in an ionization zone also leads to an explanation of the rapid termination of current runaway, i.e. the transition from rapidly increasing to more-or-less constant current for long HiPIMS pulses. Ionization is limited by the availability of neutrals as well as electrons. Four scenarios of limitation are conceivable: (i) the atom supply is limited: locally, all neutrals are already ionized; (ii) neutrals are present, but there is an insufficient supply of energetic electrons to ionize them; (iii) there is an electron confinement limitation: in the region of a strong density gradient, $dn_e/d\xi$, electrons are ejected away from the target by a strong local $\mathbf{E}_\xi \times \mathbf{B}$ drift (see observation of striations[2] or jets[9,10]), and (iv) the plasma evolution is pressure limited: the plasma will expand when the kinetic plasma pressure exceeds the magnetic pressure, i.e., when

$$\beta_{confinement} = \frac{\sum_p n_p k T_p}{\left(B^2 / 2\mu_0\right)} > 1, \tag{12}$$

where the summation is over all particles, and $\mu_0 = 4\pi \times 10^{-7}$ Vs/Am is the permeability of free space. The last point is a condition for the ultimate limit of plasma density in a magnetron. Assuming a quasi-neutral dense plasma region with a high degree of ionization, we find

$$n_e \approx \frac{B^2}{4\mu_0\, kT} \approx 4\times 10^{21}\,\mathrm{m}^{-3} \tag{13}$$

as the limit when magnetic confinement breaks down. If we assume that the plasma density at the region of strong ionization approaches $\sim 4\times 10^{21}\,\mathrm{m}^{-3}$, and the axial drift velocity of jets[10] from the target is about 2 x 10^4 m/s, we arrive at a local axial current density $j_e = en_e v_e \approx 1.2\times 10^7\,\mathrm{A/m}^2$. Based on imaging results, a dense plasma zone with the strong gradient $dn_e/d\xi$ has an electron-emitting area of about $A_{IZ} \approx 10\,\mathrm{mm}^2$, leading to a maximum current in one jet of about $I_{jet} = j_e A_{IZ} = 120\,\mathrm{A}$, which appears to be a reasonable value given that several ionization zones and jets exist simultaneously. However, this ultimate limit cannot be the one that terminates the current runaway phase because criterion (13) does not depend on the applied voltage and other conditions, whereas the leveling off to a high steady-state current for long pulses is dependent on the applied voltage.[7,8] Therefore, one or more of the other limitation scenarios must play an important role.

As shown in ref.[10], energetic electrons have a high probability to cause one or more collisions when arriving at an ionization zones. They are unlikely to simply traverse it. The azimuthal current is $I_{Hall} = en_e v_{e\xi} A$, where $v_{e\xi}$ is the electron drift velocity along the racetrack at location ξ, and A is an effective cross section of the Hall current region. As the electron

density increases in an ionization zone, the velocity $v_{e\xi}$ should decrease to keep the Hall current constant. However, each electron has the same drift velocity, given by the **E** and **B** fields and regardless of its energy, which seems to suggest that the Hall current would locally increase as the plasma density increases. The solution to this puzzle is simple when considering that the plasma must remain quasi-neutral. As the ions are removed from the ionization zone, so must be the electrons. The removal of electrons from the dense plasma zones away from the target is consistent with the experimental images of jets leaving the ionization zones. As the ionization zone develops, the gradient $dn_e/d\xi$ and associated electric field component $\mathbf{E}_\xi$ increases,[10]

$$m_e v_{e\xi} \frac{\partial v_{e\xi}}{\partial \xi} = -eE_\xi . \tag{14}$$

This increasingly removes electrons from the near target zone by the $\mathbf{E}_\xi \times \mathbf{B}$ drift and less ionization can be caused by them. Here we have a mechanism of *negative* feedback, which stabilizes the system. The stronger the ionization and $dn_e/d\xi$ the more electrons are removed from the ionization zone. This mechanism becomes important when the local E_ξ field becomes comparable to the E_z component that usually governs the electric field of the magnetic presheath. The electron jets from the near target zone fulfill important functions namely they maintain the condition of plasma quasi-neutrality as ions are evacuated from the ionization zone and they enable the observed high HiPIMS discharge currents.

This contribution is concluded by another look at the power density. In the literature, the peak power density is often nominally described as the peak current times the target potential (relative to a grounded anode) divided by the whole target area. Such nominal peak power density can be used to formally compare systems but it is unsuitable to address the plasma physics of HiPIMS. Given the highly localized nature of the plasma and current density distribution over the racetrack, the actual power density may exceed the nominal by more than one order of magnitude. For example, looking at the situation shown in Fig. 1, the peak current reaches about 100 A at an applied voltage of 500 V, and the effective area of dense plasma is only about 10^{-4} m^2, leading to a peak power density of 5×10^8 W/m^2, or about 10^9 W/m^2 in the densest plasma regions. Such high power density is related to the formation of dense plasma, which in turn insures that atoms traveling from the target have a very high probability to be ionized as they encounter a traveling dense ionization zone. Localization of power and plasma densities is therefore an essential feature of HiPIMS.

Pavel Ni and Albert Rauch are gratefully acknowledged for being key on imaging the ionization zones shown in Fig. 1. I thank Rueben Mendelsberg for his comments. This work was supported by the Assistant Secretary for Energy Efficiency and Renewable Energy, Office of Building Technology of the U.S. Department of Energy (DOE) under Contract No. DE-AC02-05CH11231.

References

[1] V. Kouznetsov, K. Macak, J. M. Schneider, U. Helmersson, and I. Petrov, Surf. Coat. Technol. **122,** 290 (1999).

[2] A. Ehiasarian, in *Plasma Surface Engineering Research and its Practical Applications*, edited by R. Wei (Research Signpost, Kerala, India, 2008), p. 35.

[3] J. T. Gudmundsson, N. Brenning, D. Lundin, and U. Helmersson, J. Vac. Sci. Technol. A **30,** 030801 (2012).

[4] M. Wright and T. Beardow, J. Vac. Sci. Technol. A **4,** 388 (1986).

[5] S. Mahieu, W. P. Leroy, D. Depla, S. Schreiber, and W. Möller, Appl. Phys. Lett. **93,** 061501 (2008).

[6] S. Kadlec and J. Musil, Vacuum **47,** 307 (1996).

[7] A. Anders, J. Andersson, and A. Ehiasarian, J. Appl. Phys. **102,** 113303 (2007).

[8] A. Anders, J. Čapek, M. Hála, and L. Martinu, J. Phys D: Appl. Phys. **45,** 012003 (2012).

[9] A. Kozyrev, N. Sochugov, K. Oskomov, A. Zakharov, and A. Odivanova, Plasma Physics Reports **37,** 621 (2011).

[10] A. Anders, P. Ni, and A. Rauch, J. Appl. Phys. **111,** 053304 (2012).

[11] A. P. Ehiasarian, A. Hecimovic, T. de los Arcos, R. New, V. Schulz-von der Gathen, M. Böke, and J. Winter, Appl. Phys. Lett. **100,** 114101 (2012).

[12] F. F. Chen, *Plasma Physics and Controlled Fusion* (Plenum Press, New York, 1984).

[13] A. Rauch, R. Mendelsberg, J. M. Sanders, and A. Anders, J. Appl. Phys. **111,** 083302 (2012).

[14] J. W. Bradley, S. Thompson, and Y. A. Gonzalvo, Plasma Sources Sci. Technol. **10,** 490 (2001).

[15] P. Sigmund, Phys. Rev. **184,** 383 (1969).

[16] M. W. Thompson, Phil. Mag. **18,** 377 (1968).

[17] Y. Yamamura and H. Tawara, Atomic Data and Nuclear Data Tables **62,** 149 (1996).

[18] D. J. Christie, J. Vac. Sci. Technol. A **23,** 330 (2005).

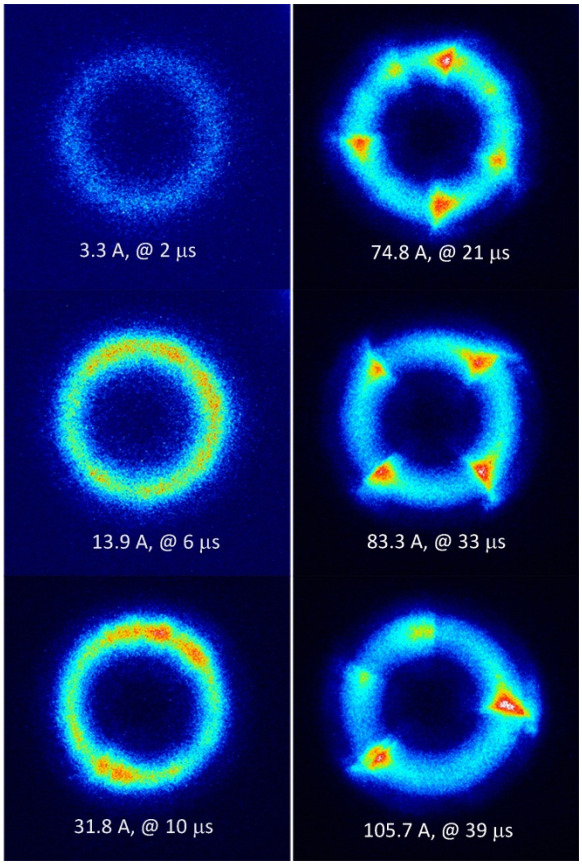

FIG. 1. Examples of counter-clockwise moving ionization zones imaged by a gated, intensified camera with an exposure time of 10 ns. Limited by the single-image capability of the camera, each image was recorded using emitted light from a different HiPIMS pulse (3" disk Al target, in 0.27 Pa Ar). The light intensity is expressed by false color. The current pulse shape is triangular, i.e. a higher current implies that the image was taken at a later time, as indicated, where $t = 0$ is the time when the current rise was clearly discernible (11 μs after applying the voltage). For more details see ref. 10.